7A.5

PATTERN: ADVANTAGES OF HIGH-RESOLUTION WEATHER RADAR NETWORKS

Katharina Lengfeld[1]*, Marco Clemens[1], Hans Münster[2] and Felix Ament[1]
[1] Meteorological Institute, University of Hamburg, Germany
[2] Max-Planck-Institute for Meteorology, Hamburg, Germany

1 INTRODUCTION

Precipitation plays an important role in driving the hydrological and the energy cycle of the lower atmosphere. For hydrometeorological applications, e.g. flood forecasting and risk management, high-resolution precipitation observations are needed to gain detailed insight in rainfall-runoff processes. Common radar systems as used in nationwide networks generally operate at S- or C-band wavelength with spatial resolution in the order of kilometers and temporal resolution of about 5 minutes. These systems cannot meet all present and future requirements. The requested spatial and temporal resolution for hydrometeorological applications is 0.1 km and 1 min, respectively (Einfalt, 2003). Therefore, radar systems capable of producing reliable and accurate precipitation estimates at high temporal and spatial resolution are required.

High-resolution weather radar (HRWR) systems have been developed in recent years that operate in the X-band frequency range and are capable of scanning precipitation with spatial resolution of 60 m and temporal resolution of 30 s. Recent studies (Lengfeld et al. (2012) and Trabal et al. (2013)) support observations at X-band frequencies as an alternative or an addition to S- and C-band, e.g in regions, where S- and C-band radars are blocked by mountains. Besides higher resolution, these systems are cost-effective compared to S- or C-band radars because of smaller antenna size (Bringi et al., 1990). Disadvantages of single X-Band radars are relatively short range and large influence of attenuation by liquid water (e.g. Atlas and Banks (1951); Gunn and East (1954); Wexler and Atlas (1963); Dutton (1967)).

The project *Precipitation and ATTenuation Estimates from a high resolution weather Radar Network* (PATTERN) funded by the German Research Foundation (DFG) intends to demonstrate that a network of HRWRs can overcome this apparent drawback and to identify advantages and disadvantages of the network as well as single X-band radars. In section 2, a description of the specifications of the modified HRWR systems as well as the design of the network will be given. Section 3 deals with algorithms used to derive precipitation from reflectivity measurements from single radars and algorithms exploiting the benefits of having a network, e.g. for clutter removal and replacing disturbed pixels by measurements from other radars instead of interpolating. In section 4, a comparison to measurements of weather radar operating in C-band used by the *German Weather Service* (DWD) focuses on the ability of high-resolution observations to give information about small scale structures of rain events. Section 5 gives a short summary and an outlook on future applications of high-resolution precipitation observations using X-band radar networks.

* *Corresponing author address:* Katharina Lengfeld, University of Hamburg, Meteorological Institute, Hamburg, Germany, +49 40 42838 5158, e-mail: katharina.lengfeld@zmaw.de

2 RADAR NETWORK

The *University of Hamburg* and the *Max-Planck-Institute for Meteorology* set up a network consisting of four X-band radars (*Hungirger Wolf Tower* (HWT), *Quarnstedt* (QNS), *Bekmünde* (BKM) and *Moordorf* (MOD)) in the North of Hamburg, Germany (Fig. 1).

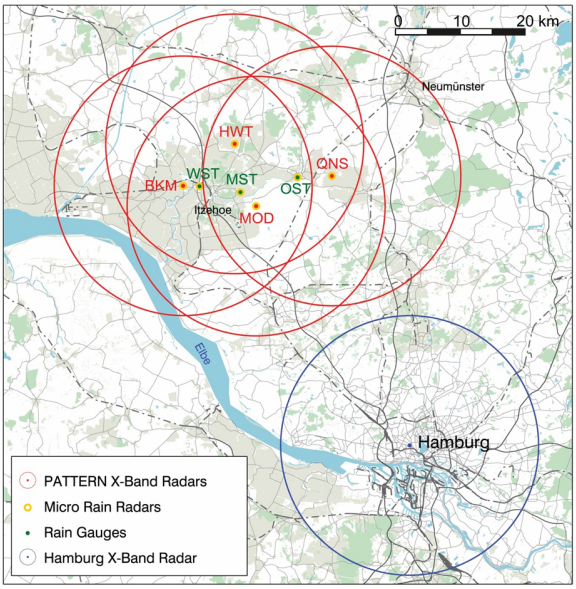

Figure 1: *Position of the four network radars Hungriger Wolf Tower (HWT), Quarnstedt (QNS), Bekmünde (BKM) and Moordorf (MOD) marked as red, the Hamburg radar marked in blue and their 20 km range. Reference stations OST, MST and WST are marked in green.*

The network is operational since January 2012. Each radar has a maximum range of 20 km. The covered region of the network is approximately 60 km x 80 km. Two neighbouring radars are at least 11 km apart, but not more than 16 km. Therefore, a large area within the network is covered by at least two radars at the border and up to four radars in the center. Micro Rain Radars (MRR) at each radar site and three reference stations consisting of MRR and rain gauge complement the network. These stations are used to calibrate and evaluate the X-band radars. An additional X-band radar is set-up at the roof of the *Meteorological Institute* of the University of Hamburg since May 2013. The whole PATTERN catchment is covered by a C-band radar operated by DWD.

The low-cost HRWRs used in PATTERN are modified ship navigation radars that bridge the gap between rain gauges and high-end long range systems as C- or S-band radars. The radar front end including scanning unit is based on a standard navigation radar (Fig. 2a). The original fan beam antenna is replaced by high gain pencil beam antenna; in order to reduce side lobes an offset parabolic dish is used. Antenna and scanning drive is protected by a low-loss radome with air conditioning. Signal processing, data management and radar control is PC-based. Technical details about the radar systems and the scanning scheme are listed in Table 1.

Table 1: *HRWR specifications*

PerformanceParameters	*Specifications*
Range Resolution	60 m
Azimuth Resolution	1°
Time Resolution	30 s
Maximum Range	20 km
Calibration Accuracy	± 1dB
Transmit Power	25 kW
Frequency	9410 MHz
Pulse Width	0.08 μs
Pulse Repitition Rate	2100 Hz
Beam Width	3°

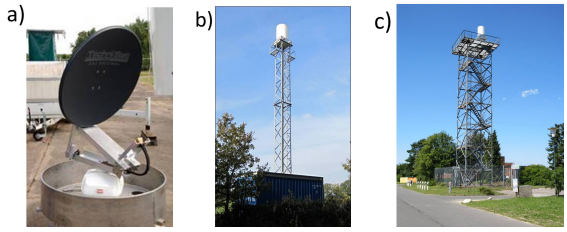

Figure 2: *Modified ship navigation radar with parabolic dish (a), typical radar tower in Quarnstedt (b) and radar at Hungriger Wolf (c).*

The radars obtain reflectivity measurements with temporal resolution of 30 s, spatial resolution of 60 m and azimuthal resolution of 1°. The scanning scheme is azimuthal only. Fixed elevation angles can be adjusted for optimum operation according to site conditions. A typical radar system consists of radar, radome, a steel tower and a container. The radars MOD, BKM and QNS are set up on a 10 m high steel tower mounted on a steel construction on the roof of a container. As an example radar QNS is shown in Fig. 2b. The whole system is 16 m high and fits into the container. Therefore, it can be moved easily compared to other radar systems. HWT is placed on an already existing steel tower at the airport *Hungriger Wolf* (Fig. 2c).

3 DATA PROCESSING

The X-band radars used in the PATTERN network operate with pulse repetition frequency of 2100 Hz. The antenna rotates with 24 rpm. Raw reflectivity signal does not only contain meteorological echoes from precipitation but also non-meteorological echoes (clutter) and background noise. Therefore, a number of correction algorithms need to be applied to the raw data in order to isolate the actual precipitation signal. Disturbances mainly caused by other radars and radio links are already elimated by comparing adjacent pulses before the reflectivities are recorded as 30 second averages. In Fig. 3a the 30 s average raw reflectivities are shown for August 3rd, 2012, 13:35 UTC for radar MOD. In the Western part of the radar image signal from precipitation is evident, in the center of the image is small scale clutter and background noise superimposes the radar image.

The low-cost X-band radars cannot observe Doppler shift neither do they perform polarimetric measurements. Therefore, state of the art methods to eliminate clutter cannot be used. Clutter detection is only based on temporal and spatial variability of reflectivity. Clutter is characterized by high reflectivity values and can be divided in two different types: Static and dynamic clutter. Static clutter is caused e.g. by trees, houses and windmills and is present in almost every data set at the same radar pixels. To eliminate this type of clutter a map is generated over ten days by counting the time steps at which reflectivity is higher than a certain threshold. Range gates with 95% high reflectivity values are marked as static clutter.

Dynamic clutter is caused by birds, insects or other radars operating in the same frequency range. For identifying dynamic clutter several algorithms are applied. The first algorithm is based on the spatial structure of the reflectivity signal,

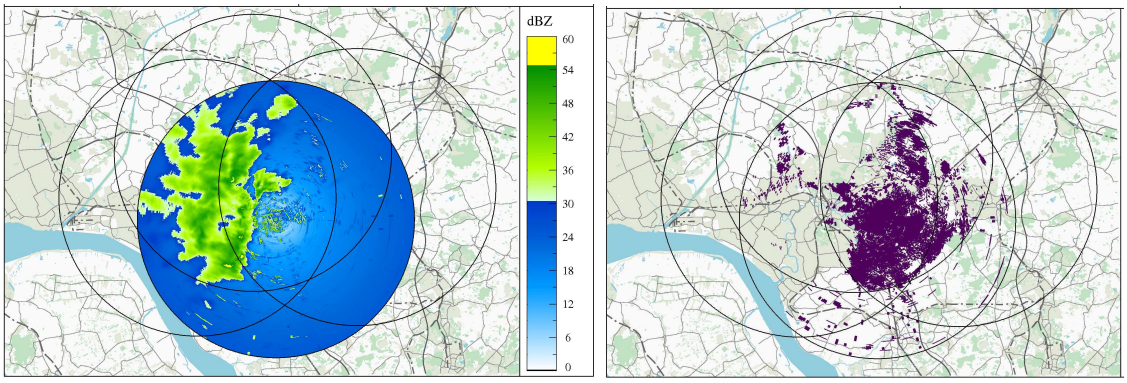

(a) *(b)*

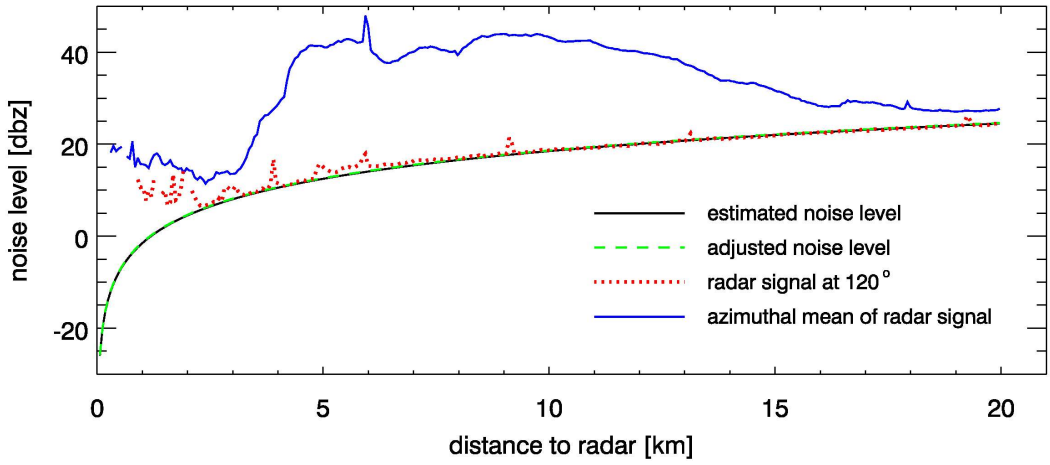

(c)

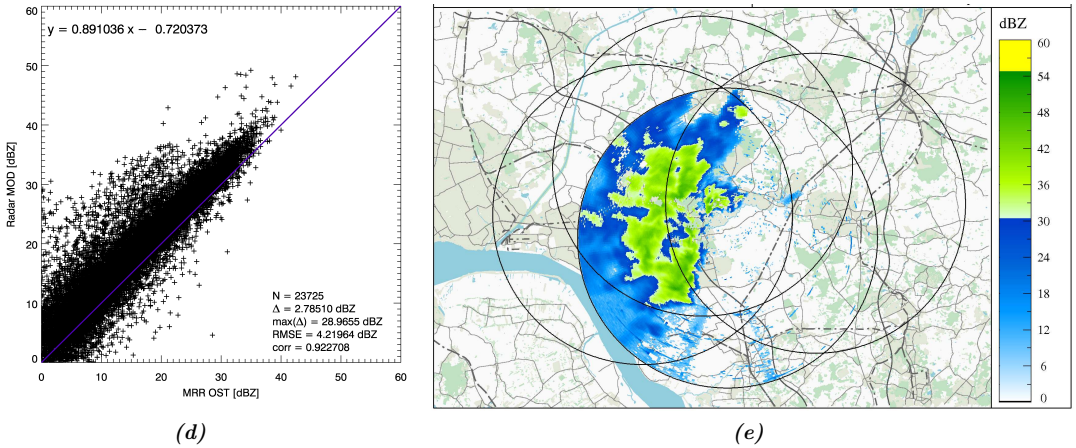

(d) *(e)*

Figure 3: *Processing reflectivity data from radar MOD for August 3rd, 2012, 13:35 UT: (a) Raw reflectivity field, (b) clutter index field, (c) noise level, (d) comparison of radar MOD and MRR OST for September 1st to November 30th, 2012, with number of events (N), mean bias (Δ), maximum bias, root mean square error (RMSE) and correlation (corr), and (e) corrected and calibrated reflectivity field*

so called texture of reflectivity (TdBZ), that is calculated from averages of quadratic reflectivity differences of neighbouring range gates (Hubbert et al., 2009). A second feature of spatial heteorogeneity is the frequency of sign changes (SPIN) in reflectivities of neighbouring range gates (Hubbert et al., 2009). Pixels are marked as dynamic clutter if both, TdBZ and SPIN, exceed an earlier de-

termined statistical threshold. Other signals, e.g. from external emitters affect whole azimuth angles or certain distances and occur in form of spikes or rings in the radar image. Spikes are characterized and identified by a sign change in difference between neighbouring azimuth angles, rings by a sign change in differences between neighbouring radar beams.

The PATTERN network has two features that can be used for further clutter detection: High temporal resolution and large overlapping areas covered by more than two radars. The high temporal resolution of 30 seconds of the PATTERN network allows for the following clutter detection method: By comparing the current radar image to the two previous time steps, range gates with high reflectivities that are only present in the current image but not in the previous ones are most likely clutter and are eliminated. The other advantage of the PATTERN network is the large area covered by more than two radars. Therefore, multiple information on reflectivity of other radars can be used to identify clutter. A map of all clutter pixels for radar MOD is shown in Fig. 3b.

The radar signal is superimposed by a noise field that consists of two different kinds of noise: Receiver noise and stochastic or speckle noise. Receiver noise is dependent on receiver temperature and distance to the radar. The HRWRs used in PATTERN cannot measured the receiver noise level. Therefore, it is determined by using a first guess to distinguish between reflectivities caused by precipitation and by noise. From the rain-free parts a noise level for the current time step is estimated and averaged with the noise level of the last 10 time steps. The noise function dependent on the distance to the radar and the estimated noise level, as well as the azimuthal mean of the radar signal and the radar signal at 120° are shown in Fig. 3c. After subtracting the noise level from the reflectivity field, precipitation signal and speckle noise still remains. To identify speckle noise, reflectivity within a three times three window around a range gate is considered. If five or more range gates have positive reflectivity values the range gate is considered as precipitation, otherwise it is elimated as speckle noise.

In order to calibrate reflectivity measurements of the X-band radars, observations from MRRs are used. Within the PATTERN region three reference stations consisting of MRR and rain gauge are operated in the overlapping area. Measurements from rain gauges are used to calibrate the MRRs. The X-band radars are calibrated by comparing reflectivity measurements of corresponding range gates to data obtained from the MRR closest to the radar. The corresponding MRR level is calculated based on the elevation angle of the X-band radar. A comparison between radar MOD and the reference station OST is depicted in Fig. 3e for September 1st until November 30th, 2012. Overall the X-band radar MOD fit the MRR OST measurements quite well with a mean bias of 2.8 dBZ and a correlation of 0.92.

As X-band frequency range is highly influenced by attenuation, an algorithm especially developed for small single-polarized X-band radars is used according to Nichol and Austin (2003). This algorithm allows for attenuation correction in real time because of its low computation time and its higher numeric stability compared to older methods (Hitschfeld and Bordan (1954) and Hildebrand (1978)). The corrected and calibrated reflectivity field is shown in Fig. 3e.

The algorithms described above are applied to all four radars. The corrected and calibrated reflectivity fields for radars BKM, HWT, MOD and BKM are shown in Fig. 4a. Many gaps are evident in the reflectivity fields of all four radars caused by clutter. For single radars these gaps are usually filled by interpolation. Therefore, information about small scale structure of the rain event gets lost. Having an overlapping network allows for filling most of the gaps with reflectivity measurements from other radars. The coverage within the network in Fig. 4b indicates that more than 99% of the network area is covered by undisturbed reflectivities observation from at least one radar. Thus, gaps can be filled without interpolation and the small scale structure of the rain event is kept as demonstrated in Fig. 4c. For the few datagaps left, interpolation is used.

In order to obtain precipitation estimates from the reflectivity fields, a common Z-R-relation is used. Composites of all four network radars are calculated on a rotated Cartesian grid with the equator shifted into the PATTERN region to allow for equidistant grid cells. Reflectivities or precipitation rates of all range gates inherent in a certain grid are averaged. The composite of the precipitation field for August 3rd, 2012, 13:35 UTC on a 250 m grid is shown in Fig. 4d.

4 COMPARISON TO C-BAND RADAR

In the last section it has been shown that several algorithms are needed to obtain undisturbed calibrated reflectivity fields from raw data for the PATTERN network. In order to give an estimation on the quality of the X-band radar products, reflectivity data is compared to the products of the radar Hamburg operated by DWD. Radar Hamburg measures reflectivity in the C-band frequency range with spatial resolution of 1 km, azimuthal resolution of 1° and temporal resolution of 5 min.

A comparison of the composite of reflectivity

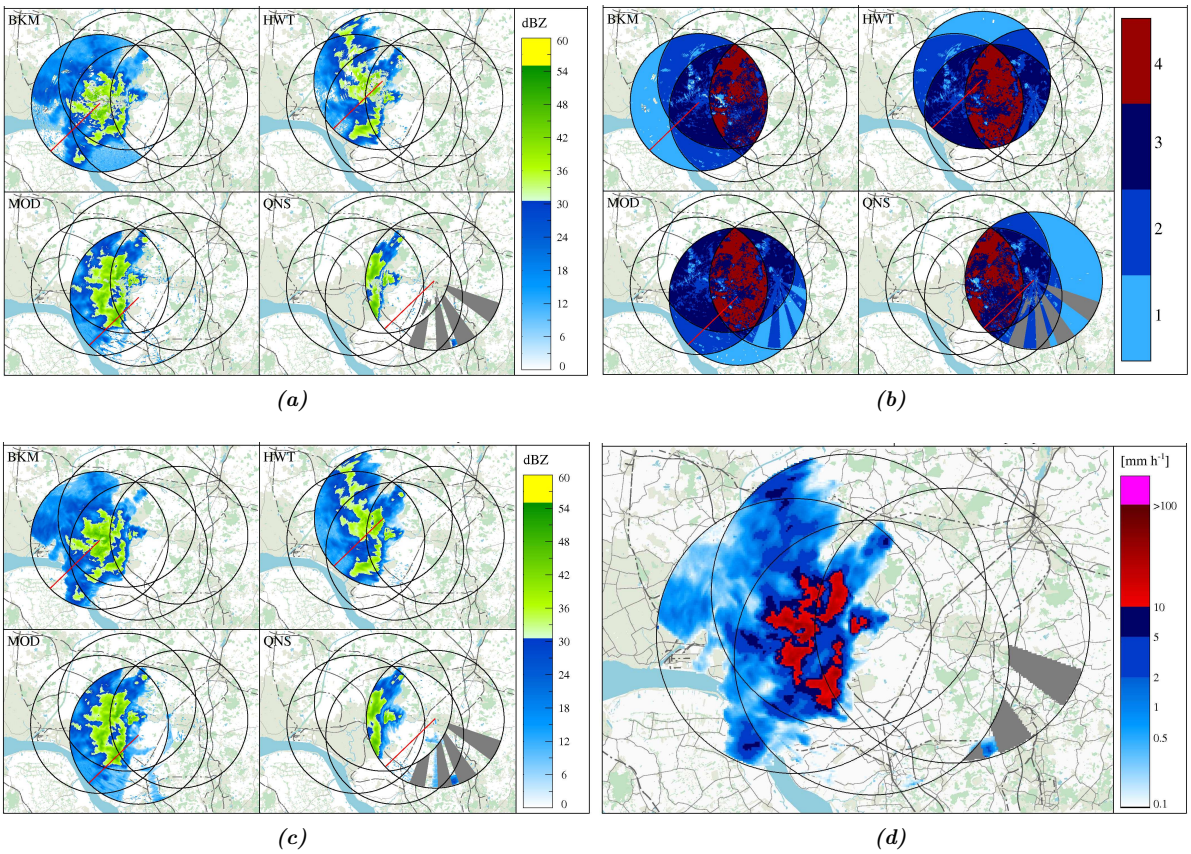

Figure 4: *(a) Corrected and calibrated reflectivity field of radars BKM, HWT, MOD and QNS for August 3rd, 2012, 13:35 UTC, (b) network coverage, (c) filled reflectivity fields and (d) precipitation composite of all four radars*

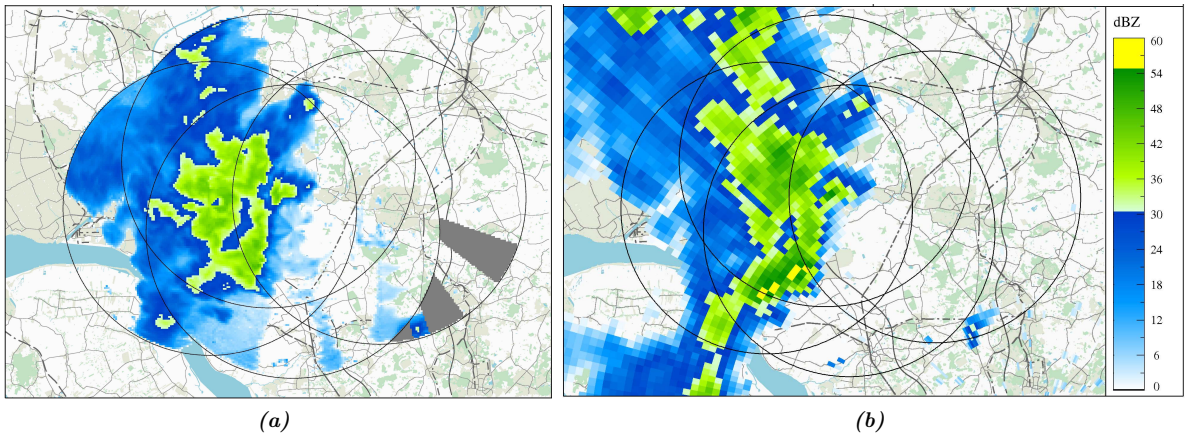

Figure 5: *((a) Composite of reflectivity fields of all for network radars for August 3rd, 2012, 13:35 UTC and (d) reflectivity field from radar Hamburg*

fields of the four PATTERN radars (Fig. 5a) to the product of radar Hamburg (Fig. 5b) for August 3rd, 2012, 13:35 UTC indicates high spatial accordance of both systems. Both, geographical position of the precipitation area as well as it's maxima, are displayed well by the PATTERN radars and radar Hamburg. The higher resolution of the PATTERN product compared to the DWD radar is particularly striking. This allows for enhanced and more detailed spatial allocation of precipitation. Nevertheless, reflectivity values are higher at radar Hamburg than in the PATTERN network.

The good agreement between PATTERN network and radar Hamburg in terms of reflectivity is also evident in a long term comparison of both systems in Fig. 6. All precipitation events that occur

between July 17th and September 30th are taken into account and reflectivity values are divided in 2 dBZ steps. Here, as well as in the comparison above, the PATTERN network slightly underestimates the reflectivities measured by radar Hamburg, but overall the PATTERN network provides reliable reflectivity data and promising results in terms of higher resolution.

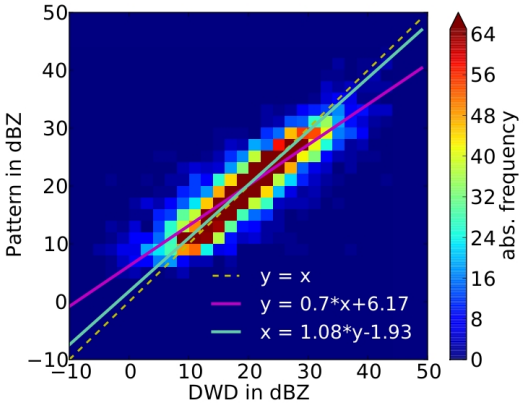

Figure 6: *Comparison of reflectivity values from radar Hamburg (abscissa) and radar MOD (ordinate) at four different range gates from July 17th to September 30st, 2012. Absolute frequency is shown in different colors from low levels in blue to high levels in red.*

5 SUMMARY & OUTLOOK

It has been shown, that the network of four low-cost high-resolution X-band radars used within the PATTERN project provide reasonable and reliable precipitation estimates in high spatial and temporal resolution. Several algorithms have been introduced to eliminate clutter and noise from raw reflectivity fields using the advantage of high temporal resolution and information of multiple radars in overlapping areas within the network. A comparison to measurements from a C-band radar operated by the DWD indicates that the PATTERN network slightly underestimates reflectivity but displays the spatial structure of rain events very well in higher resolution than nationwide radar networks can do.

The next step will be implementation of attenuation correction algorithms that use the advantage of a network (e.g. Chandrasekar and Lim (2008); Srivastava and Tian (1996) and Testud and Amayenc (1989)). Better estimation of attenuation can lead to better precipitation estimates because the relation between attenuation and precipitation is more stable than the relation between reflectivity and precipitation.

Furthermore, the fixed relation between radar reflectivity and precipitation will be replaced by a dynamic relation that will be determined operationally using measurements of the seven MRRs installed in the PATTERN catchment. This allows for an adaptation of the Z-R-relation to current weather conditions, e.g. shower, light or stratiform rain.

The high resolution products of the PATTERN network will also be used as input for rainfall-runoff simulations. Currently, hydrometeorological models use products from C- or S-band radars as input with resolution of several minutes in time and kilometers in space. The impact of higher spatial and temporal resolution on rainfall-runoff simulation will be investigated.

Acknowledgment

The authors thank the *German Weather Service* (DWD) for making products of their C-band radar network available for research purposes within the project PATTERN.

Special thanks goes to Mareike Burba for preparing the comparison of PATTERN network and DWD radar products and providing the results.

The project *Precipitation and Attenuation Estimates from a High-Resolution Weather Radar Network* is funded by the Deutsche Forschungsgesellschaft (DFG).

References

Atlas, D. and Banks, H. C. (1951). The interpretation of Microwave Reflections from Rainfall. *J. Meteor.*, 8:271–282.

Bringi, V. N., Chandrasekar, V., Balakrishnan, N., and Zrnic, D. S. (1990). An Examination of Propagation Effects in Rainfall Radar Measurements at Microwave Frequencies. *J. Atmos. Oceanic Technol.*, 7:829–840.

Chandrasekar, V. and Lim, S. (2008). Retrieval of Reflectivity in a Networked Radar Environment. *J. Atmos. Oceanic Tech.*, 25:1755–1767.

Dutton, E. J. (1967). Estimation of Radio Attenuation in Convective Rainfalls. *J. Appl. Meteor.*, 6:622–668.

Einfalt, T. (2003). A User Perspective in Germany: What is Espected by Agencies and Government from Radar Data? *Int. J. River Basin Management*, 1:1–5.

Gunn, K. L. S. and East, T. (1954). The Microwave Properties of Precipitation Particles. *Quart. J. R. Meteor. Soc*, 80:522–545.

Hildebrand, P. H. (1978). Iterative Correction for Attenuation of 5 cm Radar in Rain. *J. Appl. Meteor.*, 17:508–514.

Hitschfeld, W. and Bordan, J. (1954). Errors Inherent in the Radar Measurement of Rainfall at Attenuating Wavelengths. *J. Meteorol.*, 11:58–67.

Hubbert, J. C., Dixon, M., and Ellis, S. M. (2009). Weather Radar Ground Clutter. Part II: Real-Time Identification and Filtering. *J. Atmos. Oceanic Technol.*, 26:1181–1197.

Lengfeld, K., Clemens, M., Feiertag, N., and Ament, F. (2012). Precipitation and Attenuation Estimates from a High-Resolution Weather Radar Network (PATTERN): Design of the Experiment. In *Proc. of 7th European Conference on Radar in Meteorology and Hydrology*, Toulouse, France.

Nichol, J. C. and Austin, G. L. (2003). Attenuation Correction Constraint for Single-Polarisation Weather Radar. *Meteorol. Appl.*, 11:345–354.

Srivastava, R. C. and Tian, L. (1996). Measurements of Attenuation by a Dual-Radar Method. *J. Atmos. Oceanic Tech.*, 13:937–947.

Testud, J. and Amayenc, P. (1989). Stereoradar Meteorology: A Promising Technique for Observation of Precipitation from a Mobile Platform. *J. Atmos. Oceanic Tech.*, 6:89–108.

Trabal, J. M., Colom-Ustariz, J., Cruz-Pol, S., Pablos-Vega, G. A., and McLaughlin, D. J. (2013). Remote Sensing of Weather Hazards Using a Low-Cost and Minimal Infrastructure Off-the-Grid Weather Radar Network. *IEEE Transactions on Geoscience and Remote Sensing*, 51(5):2541–2555.

Wexler, R. and Atlas, D. (1963). Radar Reflectivity and Attenuation of Rain. *J. Appl. Meteor.*, 2:276–280.